Journal of Ovonic Research Vol. 16, No. 2, March - April 2020, p. 107 - 113

CHARACTERISTICS OF pH VARIATION ON STRUCTURAL AND OPTICAL PROPERTIES OF NANOCRYSTALLINE SnO_2 THIN FILMS BY CBD TECHNIQUE

J. F. MOHAMMAD*, M. A. A. SOOUD , S M. ABED
University of Anbar, College of education for pure Sciences, Physics Department, Iraq

Transparent nanostructure Tin dioxide (SnO_2) films with three different pH values (pH= 9, 10 and 11) were deposited on a commercial glass substrate by simple chemical bath deposition (CBD) technique, and there Structural and optical properties were characterized. The structural analysis revealed that the grown thin film exhibit tetragonal structure, small roughness and have nanocrystalline grains on the surface. While the optical results shows that the films have high transmittance (> 80 %) and the values of the optical energy gap (E_g) was 3.94, 3.84 and 3.73 eV for pH= 9, 10 and 11 respectively. These values of (E_g) greater than of bulk SnO_2 ($E_g \approx$ 3.6 eV) due to the quantum size effect.

(Received October 18, 2019; Accepted March 17, 2020)

Keywords: SnO_2 thin films, Nanostructures, CBD technique, Optical properties, AFM

1. Introduction

Many researchers have focused on modification of promising semiconductor nanomaterials in order to use in varied applications such as waveguide, light emitting nano-devices, nanoscale electronic devices and solar cells, etc. [1]. By controlling the shape and size of nanoparticle particles, we will create an attractive material with unique optical, electrical and magnetic properties [2,3]. Due to the excellent properties of Tin dioxide (SnO_2), such as, wide band gap (E_g= 3.6- 3.8 eV), high conductivity (n- type semiconductor) and high transmittance in (UV– VIS) region etc. [4-9], SnO_2 are widely used in optoelectronic devices, especially, in solar cells as a transparent conductive electrode (TCE) [10]. SnO_2 as a thin films are synthesized using various physical and chemical methods, such as, chemical vapor deposition (CVD) [11], spray pyrolysis (SP) [12], pulsed laser deposition (PLD) [13], RF magnetron sputtering (RFS) [14], Sol gel processes (SGP) [15, 16], microwave-assisted hydrothermal (MAH) [17], chemical bath deposition (CBD) [18, 19], among them, CBD technique due to inexpensive, simple and low temperature (less than 100 ºC) and good control of the growth process. The aim of this work, employ CBD technique to prepared nanocrystalline Tin oxide (SnO_2) thin films and study their structural and optical properties for solar cell applications.

2. Experimental

The high transmittance commercial glass (approximately 96%) with dimensions (2.5×2.5×0.1 cm^3) were used as substrate. The cleaning of the substrate is one of the important factors which determine the results of film surface such as homogeneity and morphology. So, initially, the slides are washed with distilled water to remove the dust, then after, they are vertically immersed in a container containing high purity acetone for 15 minutes using an ultrasonic cleaner and then dipped in chromic acid for two hours. Again rinsed with double distilled water and dried using hot air and placed in a desiccator. Using simple CBD technique, nanocrystalline SnO_2 thin films with three different values of pH (pH= 9, 10 and 11) were prepared on clean glass substrates. Stannous Chloride dehydrate ($SnCl_2.2HO_2$) of 0.1 M dissolved in 100 ml of distilled water, At 50 degrees Celsius under continuing

* Corresponding author: esp.jamalf.mohamad@uoanbar.edu.iq

stirring, a few drops of HCl were added to the solution in order to increase the solubility. Then after, 2ml of Triethanolamine as a complexing agent and 5 ml methanol were added to the solution respectively and homogeneous solution was obtained. The pH was adjusted at the required value by adding the appropriate quantity of ammonium hydroxide (NH_4OH) to the solution. Finally, an appropriate quantity of Thiourea ($CO(NH_2)_2$) of 0.1 M was added to the solution at a constant bath temperature 60 ˚C. The substrate dipped vertically in the beaker which contain the mixed solution. After deposition time of two hours, the reaction vessels were left in the chemical bath for 24 hours and then removed from the solution and washed with distilled water for several times and dried with hot air.

3. Results and discussion

3.1. Structural properties

3.1.1. XRD analysis

The X-ray diffraction (XRD) patterns of nanocrystalline SnO_2 thin films are shown in Fig. 1. From this figure, we conclude that all prepared films have polycrystalline in nature and the dominant structure was a tetragonal crystal structure with preferential orientation along (100) at 26.61º. The other peaks appear at 33.9º, 38.03º, 51.85º, 54.91º corresponding to (101), (200), (211), (220) planes which belong to the tetragonal structure, as matched with the (JCPDS card No. 88-0287). Figure 2 shows the tetragonal crystal structure of nanocrystalline SnO_2 thin film. As the pH increase (from pH=9 to pH=11), the intensity increase with small shifting to higher angles, while the full width at half maximum (FWHM) decreases which leads to decrease in grain size. The broad peaks indicate the nanosize nature of the films. Table 1 illustrates (FWHM), lattice constant, inter planers spacing and crystallite size of SnO_2. The crystallite size (D_{hkl}) is calculated using Scherrer's formula ($D_{hkl}= K \lambda /(\beta \cos\theta)$), where θ, β and λ are Bragg's angle, FWDH and wavelength of X-ray respectively [20].

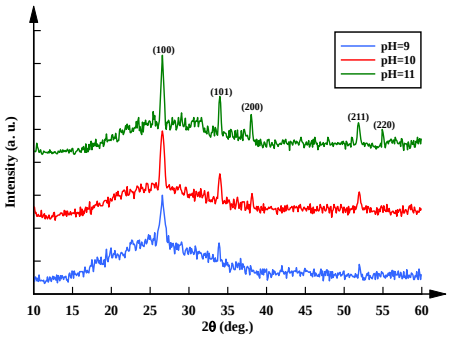

Fig. 1. XRD patterns of nancrystalline SnO_2 *thin film deposited with different pH (9, 10 and 11).*

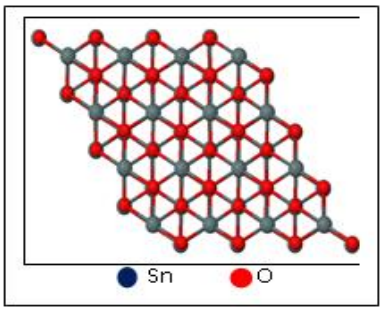

Fig. 2. Tetragonal crystal structure of nanocrystalline SnO_2 *thin film.*

Table 1. Structural parameters of noncrystalline SnO_2 *thin film.*

pH	2θ (degree)	Structure	FWHM (Degree)	Lattice constant (Å)		*hkl*	d (Å) XRD	d (Å) JCPDS	Grain size (nm)
				a=b	c				
9	26.61	Tetragonal	1.0774	4.736	3.19	110	3.348	3.347	10
10	26.64	Tetragonal	0.6785	4.741	3.189	110	3.352	3.347	16
11	26.65	Tetragonal	0.4977	4.744	3.136	110	3.354	3.347	22

3.1.2. SEM analysis

Fig. 3 displays the SEM images of the preparation samples of SnO_2 films grown on glass substrates at different pH (pH= 9, 10 and 11). In general, it can be seen that, the nanoparticles of SnO_2 have spherical shape without cluster formation and uniformly distributed over all substrates. With increasing pH in the solution the grain size of SnO_2 films increases as shown in Fig. 3. The continuous distribution of grains confirms that the grains are well adhered to the surface of the prepared films.

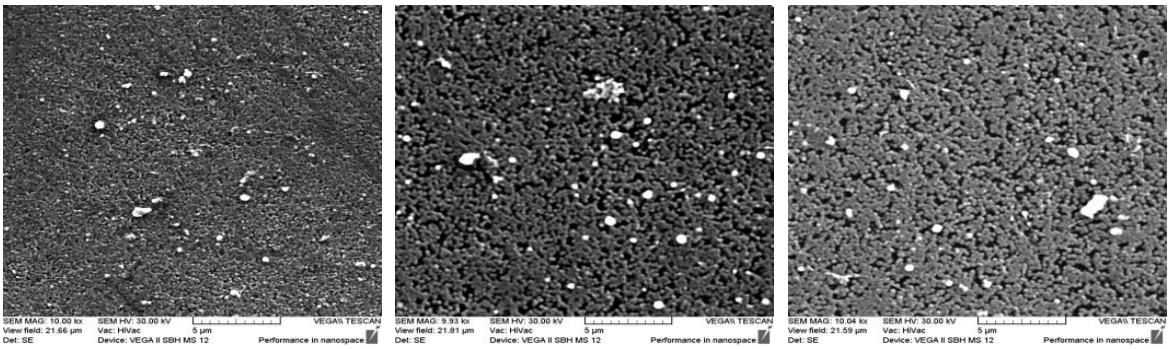

(a) (b) (c)

Fig. 3. SEM images of nanocrystalline SnO_2 *thin film: (a) - pH= 9,(b) - pH= 10, (c)- pH= 11.*

3.3.1.3. AFM Analysis

Fig. 4 shows the two and three dimensional atomic force microscopy (AFM) images. It clearly shows homogeneous distribution of grains and small roughness without voids or cracks. The surface roughness increases with increase pH in the solution of the chemical bath and this can be attributed to faster growth on the substrate.

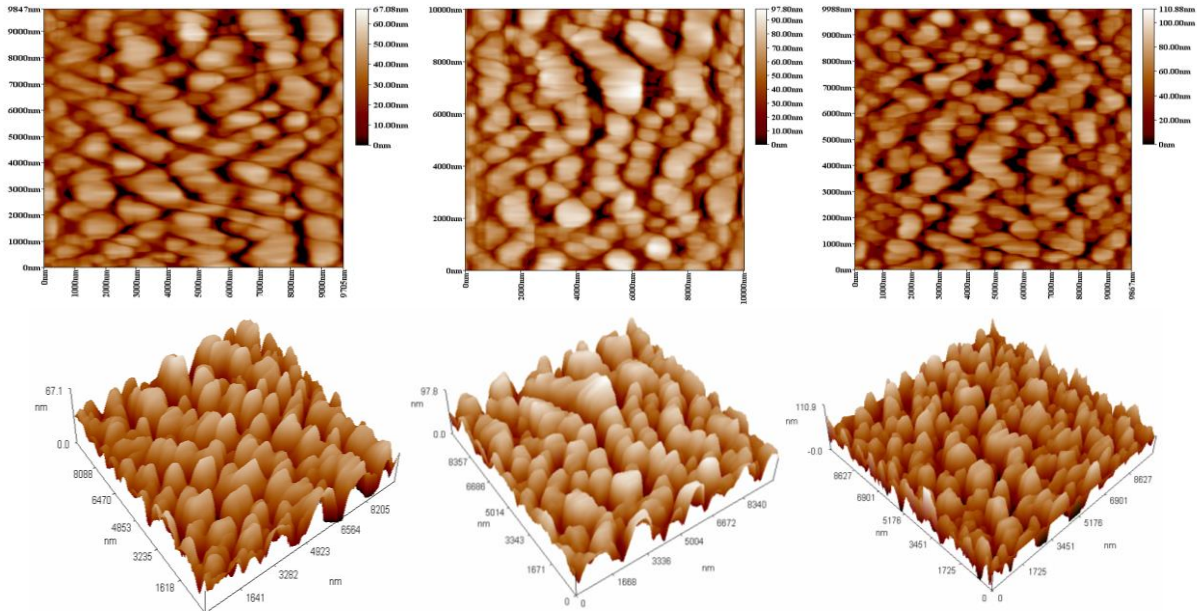

(a) (b) (c)

Fig. 4. AFM images of nanocrystalline SnO_2 thin film: (a)- pH= 9,(b)- pH= 10, (c)- pH= 11.

The good homogeneity with small roughness of the prepared films is very useful in modern applications such as solar cells. Table 2 summarizes the calculated values of surface texture of the prepared films with different pH (pH= 9, 10 and 11). The disagreement in crystal size result calculated from AFM and XRD can be ascribed to the broadening peak in XRD pattern ينشأ from strain formed in the crystal and crystal refining.

Table 2. Calculated values of nanocrystalline SnO_2 thin films from AFM analysis.

Sample	Root mean square (nm)	Ten point height (nm)	Roughness average (nm)	Average grain size (nm)
pH=9	13.2	58.3	10.7	39.11
pH=10	21.4	93.6	17.6	54.60
pH=11	22.6	96	18.8	75.19

3.2. Optical properties

The study of transmittance versus wavelengths which play an important role in the wide range of optoelectronic applications such as solar cells. The transmittance spectrum of nanocrystalline SnO_2 thin films for three different pH values (pH=9, 10 and 11) is shown in Figure (5). All spectrums show high transmittance in the visible region (approximately > 80 %). In general, the curves has a good uniform due to the high homogeneity of the film thickness on the substrate. It is evident, as the pH increase, the transmittance decreases, this is can attributed to increase in the film thickness, which can interpret as follow; the increase in nucleation and growth of grains helps to increase the formation additional Sn ions and hence combination with oxygen ions to form SnO_2 leading to increase the film thickness.

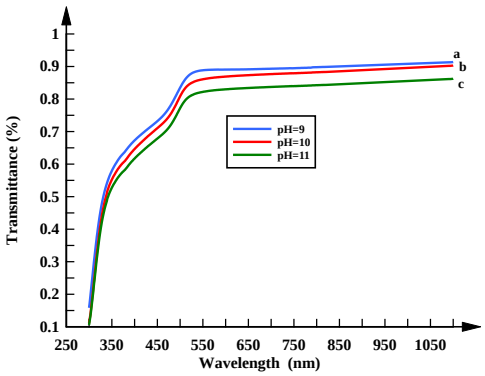

Fig. 5. Transmittance versus wavelength of nanocrystalline SnO_2 thin film: (a)- pH= 9,(b)- pH= 10, (c)- pH= 11.

The absorption coefficient (α) data can be calculated from the absorbance (A) which related with absorption coefficient by the following equation.

$$\alpha = \frac{2.3026\ A}{t} \tag{2}$$

where t– Thickness of the film. Fig. 6 shows the absorption spectra for nanocrystalline SnO_2 thin films recorded in the range (300-1100 nm) for three different pH values. At the UV- region, the films have high absorption coefficient and then decreases at different rates dependence on the film thickness to reach constant values at higher wavelengths ($\lambda > 450$), where the films become approximately transparent at this range. The absorption coefficient increases with increase pH in the chemical solution and the edge absorption shifted to higher wavelengths (red shift). The low absorption coefficient (low absorbance) is necessary for wide application in optoelectronic devices like solar cells.

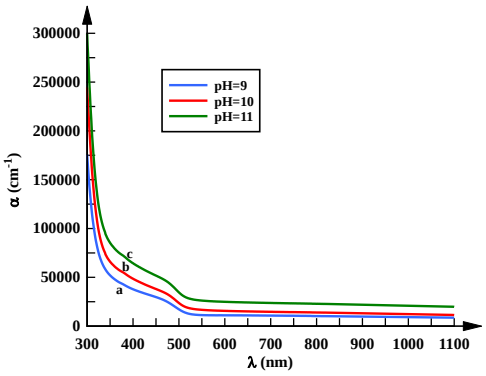

Fig. 6. Absorption coefficient versus wavelength of nanocrystalline SnO_2 thin film: (a)- pH= 9,(b)- pH= 10, (c)- pH= 11.

The optical band gap (E_g) is (are) related with absorption coefficient (α) by the following equation [21].

$$\alpha h\nu = A\,(h\nu - E_g)^n \tag{3}$$

where; (υ) is the frequency of the incident photon and (h) is Plank's constant. Fig. 7 shows direct allowed band gap (E_g) of SnO_2 films which plotted between $(\alpha h\nu)^2$ and hν (photon energy) for three different

pH (pH=9, 10 and 11). The straight portion of the graph is extrapolated to energy axis to give optical band gap. The calculated values of E_g of nanocrystalline SnO_2 thin films was 3.94, 3.84 and 3.73 eV for pH= 9, 10 and 11 respectively. The decreasing in E_g with increasing pH values is attributed to the increase in grain size and film thickness. In fact, This result related to generated allowing excitation secondary levels inside the energy gap and increase the width of these levels with the increasing pH values. As a comparison, the calculated optical band gap values are greater than of E_g of bulk SnO_2, this result attributed to the quantum size effect which related to nanoscale of grains.

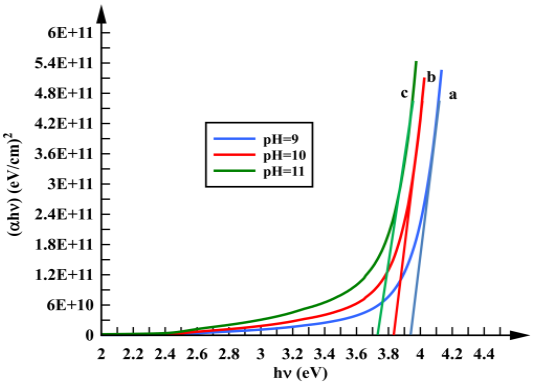

Fig. 7. Optical energy gap versus wavelength of nanocrystalline SnO_2 thin film: (a)- pH= 9,(b)- pH= 10, (c)- pH= 11.

4. Conclusions

An efficient, simpler and cheaper CBD technique successfully employed in depositing nanocrystalline SnO_2 thin films on glass substrate. The prepared films have uniform morphology and tightly adherent to the substrate. The XRD results showed that the intensity and crystallite size increase with increasing pH. The morphological results showed that the grains are well distributed over the substrate and the films have high homogeneity. Also, the prepared films have high transmittance (> 80 %) with low absorption coefficient in the visible region. The optical energy gap found to be decreased with increase pH (E_g= 3.94, 3.84 and 3.73 eV for pH= 9, 10 and 11 respectively). The high transparency and wide band gap features make these films to be suitable in nano-optoelectronic applications, especially in solar cell as a window or antireflection layer.

References

[1] S. Suresh, Nanoscience and Nanotechnology **3**, 62 (2013).
[2] Y. B. Mao, S. S. Wong, Adv. Mater **17**, 2194 (2005).
[3] A. P. Alivisatos, Science **271**, 933 (1996).
[4] A. Azam, A. S. Ahmed, S. S. Habib, A. H. Naqvi, Journal of Alloys and Compounds **523**, 83 (2012).
[5] S. Gong, J. Liu, J. Xia, L. Quan, H. Liu, D. Zhou, Materials Science and Engineering B **164**, 85 (2009).
[6] S. Li, Y. Li, Y. Wu, W. Chen, Z. Qin, N. Gong, D. Yu, Phys B: Cond. Mat. **489**, 33 (2016).
[7] B. Yuliarto, G. Gumilar, N. L.W. Septiani, Adv. Mater. Sci. Engin., 694823 (2015).
[8] L. Wang, Y. Wang, K. Yu, S. Wang, Y. Zhang, C. Wei, Sensors Actuators B **232**, 91 (2016).
[9] A. S. Ahmed, M. M. Ahafeeq, M. L. Singla, S. Tabassum, A. H. Naqvi, A. Azam, J. Luminescence **131**, 1 (2011).
[10] T. Minami, Semicond Sci. Technol. **20**, S35 (2005).
[11] A. Rosental, A. Tarre, A. Gerst, T. Uustare, V. Sammelselg, Sensors and Actuators B: Chemical **77**, 297 (2001).
[12] I. M. Arturo, R. A. Dwight, Thin Solid Films **483,** 107 (2005).

[13] S. Gupta, R. K. Roy, M. Pal Chowdhury, A. K. Pal, Vacuum **75**, 111 (2004).
[14] T. Minami, Journal of Vacuum Science & Technology A **17**, 1765 (1999).
[15] Q. Dong, H. Su, D. Zhang, F. Zhang, Nanotechnology **17**, 3968 (2006).
[16] S. Mishra, C. Ghanshyam, N. Ram, S. Singh, R. P. Bajpai, R. K. Bedi, Bull. Mater. Sci. **25**, 231 (2002).
[17] P. G. Mendes, M. L. Moreira, S. M. Tebcherani, M. O. Orlandi, J. Andrés, M. S. Li, N. Diaz-Mora, J. A. Varela, E. Longo, J. Nanopart. Res. **14**, 750 (2012).
[18] B. Yuliarto, G. Gumilar, D. W. Zulhendri, Nugraha, N. L. W. Septiani, Acta Physica Polonica A **131,** 534 (2017).
[19] Y. Lare, A. Godoy, L. Cattin, K. Jondo, T. Abachi, F. R. Diaz, M. Morsli, K. Napo, M. A. del Valle, J. C. Bernède, Appl. Surf. Sci. **255**, 6615 (2009).
[20] H. P. Klug, L. E. Alexander, X-ray diffraction procedures for polycrystalline and amorphous materials, Wiley, New York, 1974.
[21] S. Dimitrijev, Understanding Semiconductor Devices, Copyright by Oxford University Press, 2000.